Journal of Renewable Energy and Environment

Journal Homepage: www.jree.ir

Materials and Energy Research Center

MERC

Research Article

Comparative Analysis of Soft Shading Effects on the Performance of Full Cell, Half-Cut, and Shingle Photovoltaic Modules

Nur Lyana Jasmin Adil[a], Mohd Azlan Ismail[a]*, Arlinnie Bibiana Jalisa[a], Abel Alfeuz[a]

[a] *Department of Mechanical Engineering, Faculty of Engineering, Universiti Malaysia Sabah, 88400, Kota Kinabalu, Sabah.*

PAPER INFO

Paper history:
Received: 24 February 2025
Revised: 29 October 2025
Accepted: 11 November 2025

Keywords:
Photovoltaic,
Module,
Full Cell,
Half-Cut,
Shingle

ABSTRACT

Partial shading remains a challenge in photovoltaic (PV) systems, often leading to significant power losses and reduced module efficiency. To address this issue, manufacturers have developed various PV module designs, such as Full Cell, Half-Cut, and Shingle modules, each with distinct internal circuit configurations that influence shading tolerance. This work presents the background study and findings on these PV modules operating under different shading patterns and percentages. The experiment utilized a portable PV power meter (SEAWARD PV200) capable of storing the electrical parameters of the current-voltage (I-V) and power-voltage (P-V) curves. The experiments were conducted in Kota Kinabalu, Sabah, which features a tropical climate (elevated temperatures, high humidity levels, and a consistent amount of solar radiation throughout the year) that is ideal for solar energy production. Evaluation of the performance of the PV modules was carried out based on the I-V and P-V curves. The results indicate that the Full Cell PV module exhibited the highest maximum power (Pmax) reduction under horizontal and diagonal shading patterns (25%, 50%, and 75% shading). The Half-Cut PV module demonstrated better performance under horizontal shading patterns (25% and 50%) but experienced the highest Pmax reduction under vertical and diagonal shading patterns (50% and 75% shading). The Shingle PV module exhibited the highest Pmax reduction under vertical and diagonal shading patterns (25%, 50%, and 75% shading) but showed minimal reduction under horizontal shading patterns (25% and 50% shading).

https://doi.org/10.30501/jree.2025.505766.2268

1. INTRODUCTION

Photovoltaic (PV) modules are used to convert renewable solar energy into electricity and have become a major source of electricity in recent years (Gu et al., 2023). From 2010 to 2022, PV modules experienced rapid development globally, becoming one of the most advanced technologies in PV power generation, with a total installed capacity of 1047 GW (Baricchio et al., 2024). This notable progress is attributed to two primary factors: i) PV energy is clean, affordable and sustainable (Kumar et al., 2020); and ii) PV-based power generations are easy to install and non-polluting (Zhong et al., 2021). When installing a PV module, it is important to consider the potential power losses that reduce the overall performance of the PV module and influence its ability to generate power. The equation below shows the factors that influence the power losses of PV modules (SEDA, 2022).

$$P_{max} = P_{max\ STC} \times f_{mm} \times f_{age} \times f_{temp} \times f_g \times f_{clean} \times f_{unshade} \quad (1)$$

where
P_{max} = Maximum power of PV module
$P_{max\ STC}$ = Maximum power of PV module at STC
f_{mm} = Mismatch losses
f_{age} = Aging losses
f_{temp} = Temperature losses
f_g = Irradiance losses
f_{clean} = Soiling losses
$f_{unshade}$ = Shading losses

Based on the equation, Pmax STC is the maximum power of the PV module in Standard Test Conditions (STC). The STC include a solar irradiance rate of 1000 W/m^2, a cell temperature of 25°C (77°F), and an air mass (AM) of 1.5 (Xu et al., 2024). Power losses in PV modules are influenced by factors such as mismatch losses resulting from variations in the electrical parameters of individual solar cells within a PV array, aging of components due to environmental factors, temperature effects, such as increases in ambient temperature that reduce the voltage output of solar cells, solar irradiance, soiling, and shading (Shen et al., 2020; Ghosh et al., 2022). Among these, shading and soiling are particularly difficult to avoid since they are related to external environmental conditions. The occurrence of shading is a significant problem in terms of the efficiency of electrical energy generation, leading to an overall reduction in power output. The two main types of shading on the surface of PV modules are hard shading and soft shading (Alves et al., 2021). Hard shading, or soiling, mainly occurs when the cells of a PV module are obstructed by physical

*Corresponding Author's Email: lanz_mr@ums.edu.my (N. L. Ismail)

URL: https://www.jree.ir/article_234056.html

Please cite this article as: Adil, N. L. J., Ismail, M. A., Jalisa, A. B., & Alfeuz, A. (2026). Comparative Analysis of Soft Shading Effects on the Performance of Full Cell, Half-Cut, and Shingle Photovoltaic Modules, *Journal of Renewable Energy and Environment (JREE)*, 13(1), 76-84. https://doi.org/10.30501/jree.2025.505766.2268

objects such as moss, bird droppings, or leaves. Meanwhile, soft shading occurs when shadows from nearby trees or buildings fall on the surface of the PV module. This study focuses on analyzing the effects of soft shading on PV modules to develop strategies for mitigating its impact and improving the overall performance of PV module systems.

1.1. Shading Effects

Evaluation of the efficiency and performance of PV modules is based on the current-voltage (I-V) and power-voltage (P-V) curves (Chen et al., 2021). These curves illustrate the effects of various factors, such as solar radiation and cell temperature, on the performance of PV modules. Identification of the optimal operating voltage and current can be achieved by analyzing these curves. Manufacturers provide key parameters on these curves to guide users during the installation process. Figure 1 presents the I-V and P-V curves of a PV module under unshaded and shaded conditions.

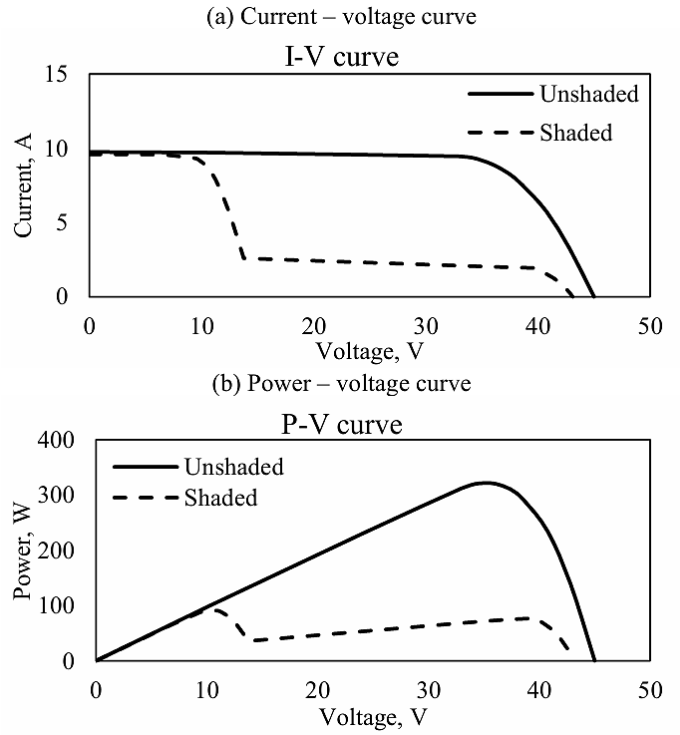

Figure 1. Example of I-V and P-V curves of the PV module under shaded and unshaded conditions

Based on Figure 1, the presence of shading causes multiple peaks in both the I-V and P-V curves due to the activation of bypass diodes, where the peaks are referred to as the global maximum power point (GMPP) and local maximum power point (LMPP). The GMPP is the highest peak on the P-V curve and represents the Pmax that the PV module can produce. Meanwhile, the LMPP is the point on the P-V curve where the PV module produces the maximum power within a specific voltage range (Pachauri et al., 2021).

1.2. PV Modules Performance Under Shading Conditions

The impact of soft shading on the performance of PV modules has been previously studied by other researchers using various methods. Chepp et al. (2021) analyzed the impact of soft shading patterns on the orientation of Full Cell PV modules. In the first scenario, the authors applied parallel shading to both the portrait and landscape orientations of the PV module. The results indicate that as shading increases row by row, the reduction in power output becomes more significant with increasing shading fraction. Conversely, when shading occurs column by column, the reduction in power output is less severe.

Next, Bhallamudi et al. (2021) analyzed the effects of soft shading on Full Cell PV modules by comparing the performance of shaded and unshaded PV modules. The authors conducted experiments under STC conditions of AM 1.5, 25˚C, and 1000 W/m². The results revealed an 80% reduction in power output between 11 a.m. and 5:30 p.m., indicating that shading can significantly affect the performance of PV modules by accelerating the reduction of Pmax.

Another investigation of soft shading was conducted by Oufettoul et al. (2023). The authors performed a simulation analysis across multiple scenarios for Full Cell PV modules. In the first scenario, the PV module was mounted in a landscape orientation, while in the second scenario, it was mounted in a portrait orientation. For both orientations, shading was applied to the bottom part of the PV module. The simulation results revealed that shading a single string in the landscape orientation resulted in a power loss of approximately 33.3% of the PV module's total capacity. Similarly, when two cell strings were shaded, the power loss escalated to 66.7%. In contrast, for the portrait orientation scenarios, shading the bottom cells of the PV module caused the P-V curve to exhibit a single peak, leading to a more significant decrease in power generation compared to the landscape orientation.

These recent studies show that research has generally focused on analyzing the effects of shading on PV modules. However, previous research has mainly concentrated on a single type of PV module, namely the Full Cell PV module. Therefore, this study provides an opportunity to perform an experimental comparison across multiple commercially available PV modules to better understand the effects of soft shading on modules with different circuit configurations.

2. EXPERIMENTAL

An outdoor experimental study was conducted to evaluate the effects of soft shading on three different types of PV modules: Full Cell, Half-Cut, and Shingle, each of which offers distinctive advantages and performance capabilities. The technical specifications of the PV modules are presented in Table 1. The experiment took place in Kota Kinabalu, Sabah, where the average global radiation is 1800 kWh/m² (Oon et al., 2020). The test was conducted between 11 a.m. and 1 p.m., when solar radiation levels were at their peak, as measured by a solar irradiance meter, ranging from 900 to 1020 W/m². The ambient temperature during the test varied from 30 to 35 ˚C. Before the experiment, the PV modules were thoroughly cleaned to remove any dust or dirt, ensuring optimal efficiency. Figure 2 illustrates the outdoor experimental setup, including the PV module, irradiance meter, temperature sensor, and PV power meter (SEAWARD PV200).

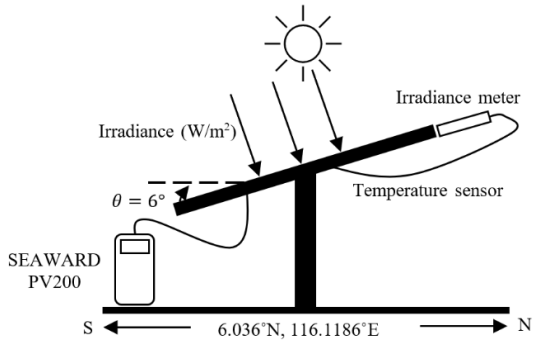

Figure 2. Outdoor experimental setup of the PV module

Table 1. Technical specifications of PV modules

Technical specifications	Full Cell	Half-Cut	Shingle
Brand	SOLAR BLUESUN	Q.ANTUM DUO	SOLAR BLUESUN
Model	BSM350M-72B	Q.PEAK DUO-G7 315-330	BSM500PM5-72SB
Cell material	72	120	432
Number of cells	Monocrystalline	Monocrystalline	Monocrystalline
Open circuit voltage	47	40.10	46.80
Short circuit current	9.6	10.04	13.40
Maximum power voltage	38.7	33.47	39.00
Maximum power current	9.09	9.57	12.82
Maximum power output	350	320	500

The irradiance meter was positioned parallel to the PV module to determine the optimal tilt angle for maximum solar irradiance, while a temperature sensor was used to monitor the PV module's temperature. The PV module was tilted at a 6-degree angle and oriented southward to align with the local latitude and maximize solar energy capture. The SEAWARD PV200 device was connected to the PV module via extension cables. Soft shading conditions were simulated using a thin film to replicate scenarios in which the PV module is partially shaded, causing power output reductions of up to 80% Bhallamudi et al. (2021). The shading effect on the PV modules was tested at percentages of 0%, 25%, 50%, and 75%, defined as the ratio of the shaded area to the total PV module area.

To compare performance under different shading conditions, the experiment included varying shading patterns—horizontal, vertical, and diagonal—for each shading percentage. The electrical responses of the PV modules, including current, voltage, and power output, were measured under different output load conditions across all defined shading percentages and patterns. The SEAWARD PV200 device recorded experimental data, including irradiation, I-V curves, and ambient temperature, which were then processed using SolarCert software and SolarDataLogger. Throughout the test, solar irradiance and temperature were continuously monitored to maintain an optimal testing environment, ensuring an accurate evaluation of the PV modules' performance.

2.1. Specifications of PV Modules

2.1.1. Full Cell PV Modules

Full Cell PV modules are constructed by connecting multiple PV cells in series. Each cell generated a small voltage, between 0.5 and 0.6 volts (Nema et al., 2010). The overall voltage output of the module increases by connecting the cells in series. In this configuration, electrical current flows consistently from the first cells to the last cell within the PV module. Depending on the power capacity of the PV module, a Full Cell PV module commonly consisted of either 60 or 72 cells arranged in a grid pattern (Tao et al., 2020). Figure 3 presents the current flow path throughout the Full Cell PV module when shaded in horizontal, vertical, and diagonal patterns.

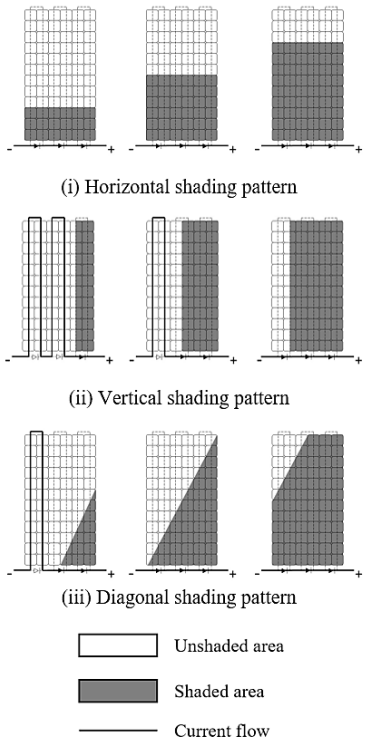

Figure 3. Electrical configuration for Full Cell PV module under different shading patterns and percentages

2.2.2. Half-Cut PV Modules

For the Half-Cut PV modules, the cells within each half of the module are connected in series, while the two halves are linked in parallel. This internal wiring configuration enhances the module's efficiency, ensuring that even if one half is shaded, the unshaded half can continue generating energy without being affected (Akram et al., 2020). Figure 4 shows the current flow path throughout the Half-Cut PV module under horizontal, vertical, and diagonal shading patterns.

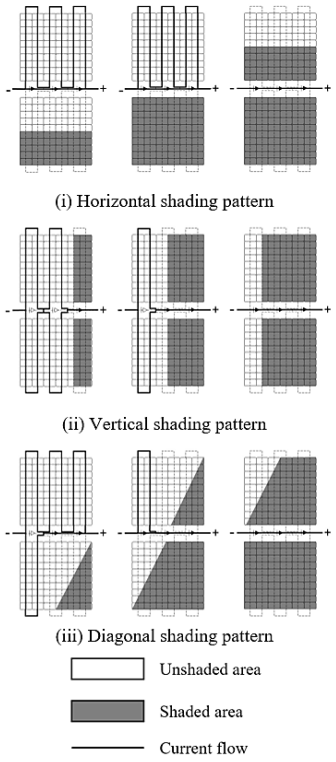

Figure 4. Electrical configuration for Half-Cut PV module under different shading patterns and percentages

2.2.3. Shingle PV Modules

Shingle PV modules are a recent innovation that feature miniature, sealed PV cells layered in an overlapping system. In these modules, the individual cells within each shingle are electrically connected in series, combining their voltages for higher power output (Oh et al., 2020). The shingles are then connected in parallel across each row of the PV module, allowing all the cells to work together efficiently. This parallel connection ensures that each shingle row functions independently, so that if one shingle is damaged or malfunctions, the rest of the PV module can continue to operate effectively. Figure 5 displays the current flow path throughout the Shingle PV module under horizontal, vertical, and diagonal shading patterns.

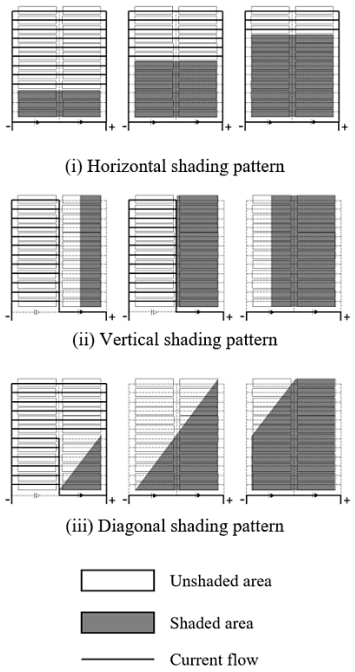

Figure 5. Electrical configuration for Shingle PV module under different shading patterns and percentages

Figures 3, 4, and 5 illustrate the electrical configuration and current flow through each PV module—Full Cell, Half-Cut, and Shingle—under various shading patterns. When shading occurs and obstructs the current flow through the strings, an alternative path is established through the bypass diodes. These diodes are strategically connected to the strings of the PV module to allow current to bypass the shaded areas, ensuring efficient operation even under partially shaded conditions.

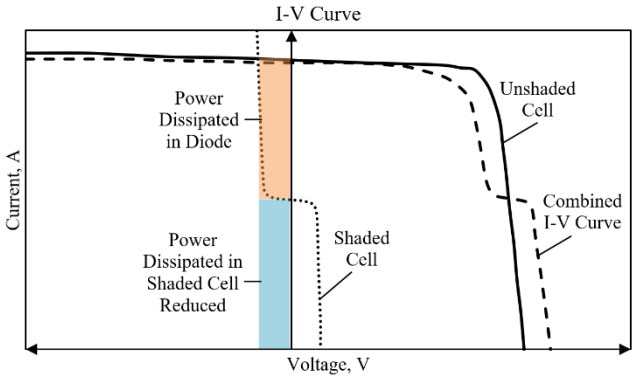

Figure 6. Example of I-V Curve of PV module cell with bypass diode

Figure 6 illustrates an example of the I-V curve of a PV module when one cell is shaded and its bypass diode is activated. Under shading, the affected cell cannot supply current at its normal voltage, so the bypass diode becomes forward biased and provides an alternate path for current. This prevents the entire module from limiting the string current but causes a voltage drop equal to the contribution of the shaded cell. The colored regions in the figure highlight energy loss: the blue area shows reduced power dissipation in the shaded cell, while the orange area represents heat loss in the bypass diode. The combined I-V curve demonstrates a reduction in peak voltage, which preserves current flow but lowers the module's overall power output and fill factor compared to the unshaded condition.

3. RESULTS AND DISCUSSION

Evaluation of the performance of the PV modules under different shading patterns and percentages was based on their I-V and P-V curves. Data collection was repeated three times for each shading condition to enhance reliability. The accuracy of the experimental data was assessed using average values and the corresponding standard deviations. A smaller standard deviation indicates higher accuracy and less variability in the experimental data. Overall, the experiment demonstrated exceptional performance, with an average accuracy exceeding 98% and relatively low standard deviations ranging from ±0.00 to ±0.24 for each data point. The shading conditions and environmental data, including solar irradiance and PV module temperature for the Full Cell, Half-Cut, and Shingle PV modules, are presented in Tables 2, 3, and 4.

3.1. Full Cell PV Module

Figure 7 presents the (a) I-V and (b) P-V curves of the Full Cell PV module under various shading conditions: (i) horizontal, (ii) vertical, and (iii) diagonal patterns, with different shading percentages (0%, 25%, 50%, and 75%). Based on Figure 7(b), for each shading pattern, the Pmax output reached 321 W under an irradiance of 919 W/m², which is approximately 8% lower than the Pmax STC value of 350 W. A decline in performance was observed when the PV module was shaded, with horizontal shading causing a substantial reduction, as shown in Figure 7(i,b). At 25% horizontal shading, Pmax dropped to 76 W, while 50% and 75% shading further reduced it to 70 W and 55 W, respectively. In contrast, vertical shading in Figure 7(ii,b) resulted in a steady decrease in power output corresponding to the increase in shading percentage. Diagonal shading in Figure 7(iii,b) exhibited a more pronounced impact, particularly at 50% and 75% shading levels, where the power output dropped significantly. These findings are consistent with those reported by Oufettoul et al. (2023), who also observed a reduction in power generation under horizontal shading for Full Cell PV modules, particularly when the modules were oriented in portrait mode. The performance loss in Full Cell PV modules under shading patterns is primarily attributed to their electrical configuration. Full Cell PV modules are constructed with PV cells connected in series. When part of the module is shaded, particularly under horizontal shading, the current flow through the shaded cells is obstructed, resulting in a significant drop in the Pmax value (Ismail et al., 2023). These findings highlight the importance of minimizing shading on PV modules to maintain efficiency. Proper installation and orientation of PV modules can help reduce the impact of shading and maximize energy generation.

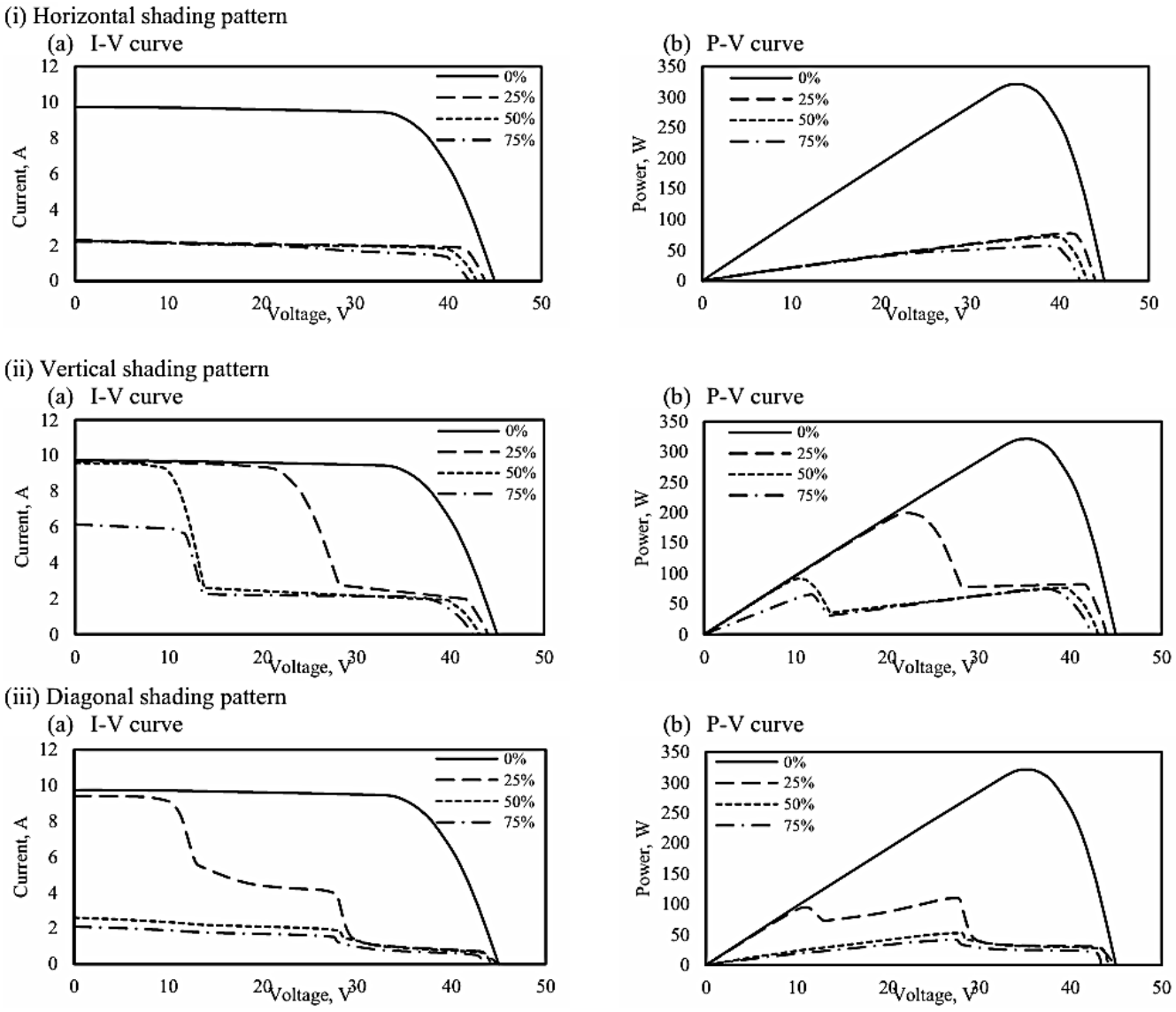

Figure 7. I-V and P-V curves for Full Cell PV module under (i) horizontal, (ii) vertical, and (iii) diagonal shading pattern

3.2. Half-Cut PV module

Figure 8 illustrates the (a) I-V and (b) P-V curves of the Half-Cut PV module under three shading patterns: (i) horizontal, (ii) vertical, and (iii) diagonal, with varying shading percentages (0%, 25%, 50%, and 75%). These findings highlight the sensitivity of the Half-Cut PV module's performance to different shading conditions, emphasizing the need for careful consideration of shading in real-world applications to optimize energy yield.

Based on Figure 8(b), the Pmax value of the Half-Cut PV module without any shading (0% shading) is 302 W, which is 5.6% lower than the actual Pmax STC value. When the PV module is subjected to horizontal shading, Figure 8(i,b) shows that the Pmax value drops to 182 W, 181 W, and 37 W for 25%, 50%, and 75% shading, respectively. The significant decrease in Pmax value for 75% horizontal shading is due to both sections of the PV module being shaded, affecting each string of the PV module cells.

Next, based on Figure 8(ii,b), when the PV module is subjected to vertical shading, the Pmax value drops to 198 W, 88 W, and 64 W for 25%, 50%, and 75% shading, respectively. The substantial decrease in Pmax value for 50% and 75% vertical shading is due to two to three PV module cell strings being shaded in both sections of the Half-Cut PV module.

For the Half-Cut PV module subjected to diagonal shading, Figure 8(iii,b) shows that the Pmax value drops to 208 W, 66 W, and 59 W for 25%, 50%, and 75% shading, respectively. For 50% and 75% diagonal shading, both sections of the PV module are affected by shading, with only one PV module string remaining unaffected when 50% diagonal shading occurs. Similar to the Full Cell PV module, the reduction in Pmax value for the Half-Cut PV module under shading conditions is due to its electrical configuration. This PV module is constructed with two sections that are electrically connected in parallel, with each string in each section connected in series. This configuration allows the PV module to maintain some level of performance even when partially shaded. For example, if an installation site is prone to horizontal shading, the optimal orientation for Half-Cut PV modules is portrait orientation. In this setup, shading the bottom half of the PV module only affects the lower section of the PV module, allowing the upper section to continue generating power. This strategic orientation helps to mitigate the impact of shading and optimize the energy yield of the PV module.

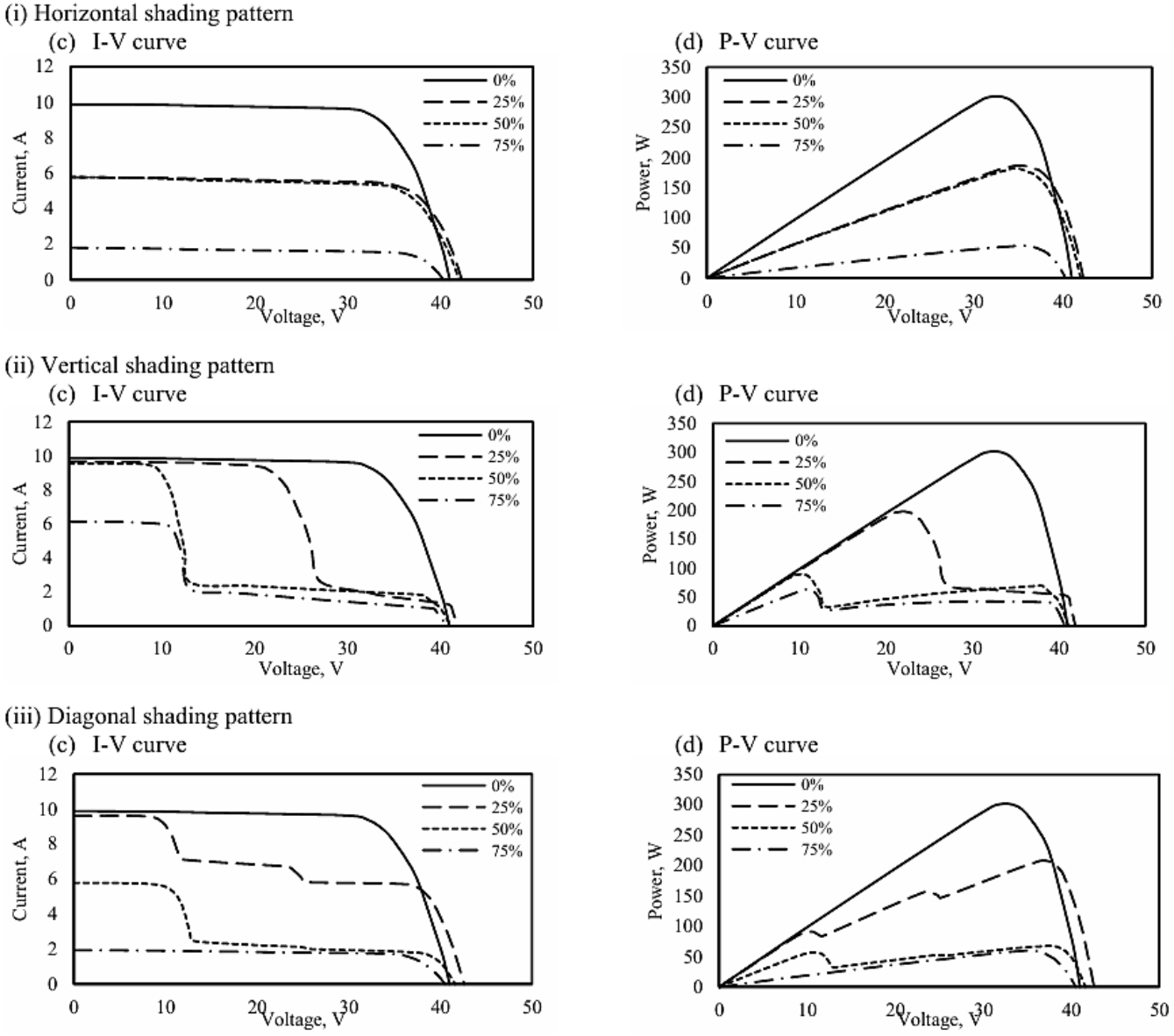

Figure 8. I-V and P-V curves for Half-Cut PV module under (i) horizontal, (ii) vertical, and (iii) diagonal shading pattern

3.3. Shingle PV module

Figure 9 shows the (a) I-V and (b) P-V curves for the Shingle PV module when subjected to (i) horizontal, (ii) vertical, and (iii) diagonal shading patterns, with multiple shading percentages (0%, 25%, 50%, and 75%). In the absence of shading (0%), Figure 9(b) shows that the Pmax value decreases to 475 W, representing a 5% reduction compared to the Pmax STC value of 500 W. When subjected to horizontal shading patterns, Figure 9(i,b) reveals that the Pmax value decreases to 301 W, 199 W, and 117 W for shading percentages of 25%, 50%, and 75%, respectively. Although the Pmax losses are significant with increasing shading percentages, the losses are relatively less severe.

The Shingle PV module's cells are interconnected in series within each row, and the rows are connected in parallel, allowing current to bypass shaded regions when part of a row is shaded. Figure 9(ii,b) demonstrates that the Pmax values of the Shingle PV module decrease to 90 W, 58 W, and 56 W for 25%, 50%, and 75% shading under vertical shading patterns. This reduction in Pmax value is attributed to vertical shading disrupting entire columns of cells. Since Shingle PV modules utilize parallel-connected rows, shading a column significantly reduces the Pmax value. In Figure 9(iii,b), the Pmax value decreases to 207 W, 82 W, and 48 W for 25%, 50%, and 75% shading under diagonal shading patterns. Diagonal shading patterns impact multiple rows and columns unevenly. At 25% diagonal shading, parallel connections between rows partially mitigate losses by rerouting current through unaffected rows. However, at 50% and 75% diagonal shading, each row of the Shingle PV module is affected, causing a significant drop in the Pmax value. To mitigate the reduction in Pmax value due to shading for Shingle PV modules, it is recommended to position the PV modules to minimize exposure to vertical and diagonal shading. For instance, installations should avoid alignments near tall structures or trees.

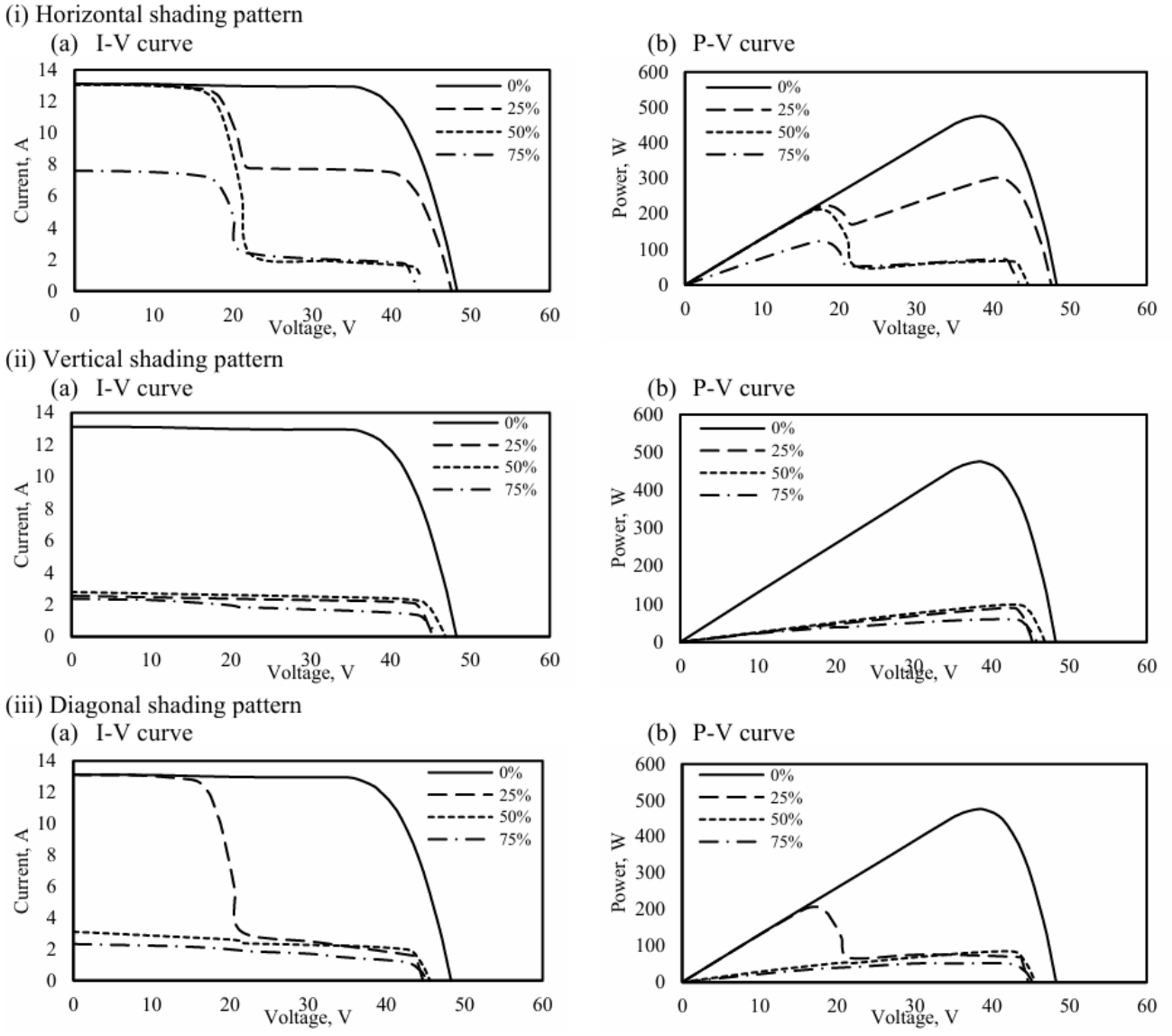

Figure 9. I-V and P-V curves for Shingle PV module under (i) horizontal, (ii) vertical, and (iii) diagonal shading pattern

3.4. Comparison Between Percentage of Power Reduction

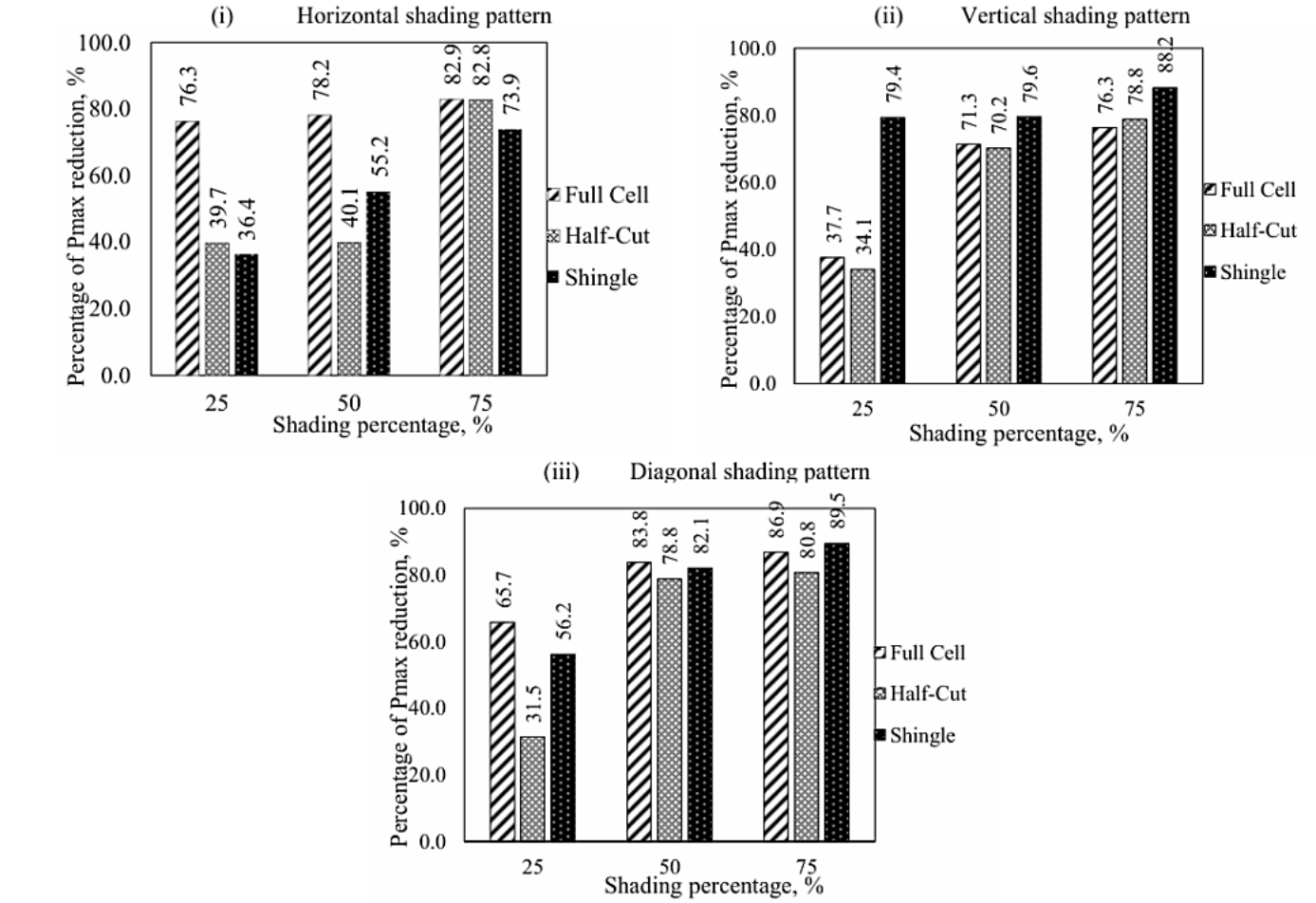

Figure 10. Percentage of power reduction for (i) horizontal shading, (ii) vertical shading, and (iii) diagonal shading for Full Cell, Half-Cut, and Shingle PV modules

Figure 10 presents a comparative analysis of the percentage reduction in Pmax for (i) horizontal, (ii) vertical, and (iii) diagonal shading patterns across Full Cell, Half-Cut, and Shingle PV modules. From Figure 10(i), it is evident that the Full Cell PV module experiences the most significant reduction in Pmax under horizontal shading patterns (25%, 50%, and 75% shading), followed by the Shingle PV module, while the Half-Cut PV module exhibits the least reduction (25% and 50% shading). In Figure 10(ii), the Shingle PV module shows the highest Pmax reduction across all shading levels (25%, 50%, and 75%), followed by the Full Cell PV module. The Half-Cut PV module shows the lowest Pmax reduction only at the 25% shading level. Next, Figure 10(iii) shows that under the diagonal shading pattern, both Full Cell and Shingle PV modules exhibit the highest Pmax reduction, with the Half-Cut PV module showing a lower reduction only at the 25% shading level. When comparing soft and hard shading effects on PV modules, hard shading has a much more severe impact. For example, a study by Ismail et al. (2023) highlights that hard shading can lead to a complete loss of Pmax output (0 W) when each string of the PV module is entirely shaded. This occurs because hard shading completely blocks sunlight from reaching the cells. This comparison underscores the importance of selecting the appropriate PV module based on shading pattern and percentage. Half-Cut PV modules are better suited for partially shaded environments, whereas Full Cell and Shingle PV modules should be installed in areas with minimal shading to maximize energy generation.

5. CONCLUSIONS

This study provided a comparative evaluation of soft shading effects on Full Cell, Half-Cut, and Shingle PV modules, emphasizing how internal circuit configurations influence shading tolerance. The results indicate that the Full Cell PV module exhibits the highest sensitivity to horizontal shading, with a substantial reduction in power output due to its series-connected cell strings, which restrict current flow when shaded. Conversely, the Half-Cut PV module demonstrates greater resilience to shading, particularly under horizontal shading patterns. This improved performance is attributed to its two-section construction, where each section operates independently, enabling continuous power generation. The Shingle PV module, characterized by its overlapping cell arrangement and parallel connections between shingle rows, is less affected by horizontal shading but experiences notable power losses under vertical and diagonal shading patterns. Across all three PV module types, the percentage of power loss increases with shading percentage, with diagonal shading exerting the most severe impact. These findings underscore the importance of selecting appropriate module types and installation orientations during the early stages of PV system design. Early decisions on PV module selection and layout can reduce shading losses and improve overall energy yield. For instance, in areas prone to horizontal shading, installing Half-Cut PV modules enhances performance by allowing each half of the module to operate independently. In environments exposed to vertical or diagonal shading, installing Shingle PV

modules can reduce power loss since the cells are connected in series within each shingle and the rows are arranged in parallel. By optimizing PV module positioning and minimizing exposure to shading sources, system efficiency can be maximized, leading to improved energy yield and overall system performance. Future research could further explore mitigation strategies, such as optimized bypass diode placement and adaptive tracking systems, to enhance PV module efficiency under varying shading conditions.

ACKNOWLEDGEMENT

The authors sincerely thank all the organizations that provided valuable data for this study.

REFERENCES

1. Akram, M. W., Li, G., Jin, Y., Zhu, C., Javaid, A., Akram, M. Z., & Khan, M. U. (2020). Study of manufacturing and hotspot formation in cut cell and full cell PV modules. *Solar Energy, 203*, 247-259. https://www.sciencedirect.com/science/article/pii/S0038092X2030437

2. Alves, T., Torres, N., Marques Lameirinhas, J. P., & Fernandes, C. A. F. (2021). Different techniques to mitigate partial shading in photovoltaic panels. *Energies, 14*(13), 3863. https://www.mdpi.com/1996-1073/14/13/3863

3. Baricchio, M., Korevaar, M., Babal, P., & Ziar, H. (2024). Modelling of bifacial photovoltaic farms to evaluate the profitability of East/West vertical configuration. *Solar Energy, 272*, 112457. https://www.sciencedirect.com/science/article/pii/S0038092X24001518

4. Bhallamudi, R., Kumarasamy, S., & Sundarabalan, C. K. (2021). Effect of dust and shadow on performance of solar photovoltaic modules: experimental analysis. *Energy Engineering, 118*(6), 1827-1838. https://cdn.techscience.press/ueditor/files/energy/TSP_EE-118-6/TSP_EE_16798/TSP_EE_16798.pdf

5. Chen, Z., Yu, H., Luo, L., Wu, L., Zheng, Q., Wu, Z., et al. (2021). Rapid and accurate modeling of PV modules based on extreme learning machine and large datasets of IV curves. *Applied Energy, 292*, 116929. https://www.sciencedirect.com/science/article/pii/S0306261921004098

6. Chepp, E. D., & Krenzinger, A. (2021). A methodology for prediction and assessment of shading on PV systems. *Solar Energy, 216*, 537-550.

7. Ghosh, S., Roy, J. N., & Chakraborty, C. (2022). A model to determine soiling, shading and thermal losses from PV yield data. *Clean Energy, 6*(2), 372-391. https://www.sciencedirect.com/science/article/pii/S0038092X21000050

8. Gu, Q., Li, S., Gong, W., Ning, B., Hu, C., & Liao, Z. (2023). L-SHADE with parameter decomposition for photovoltaic modules parameter identification under different temperature and irradiance. *Applied Soft Computing, 143*, 110386. https://www.sciencedirect.com/science/article/pii/S1568494623004040

9. Ismail, M. A., Adil, N. L. J., Yan, F. Y., Amaludin, N., Bohari, N., & Sar-ee, S. (2023). Analysis of the Effects of Hard Shading Pattern on I–V Performance Curve. *Applied Solar Energy, 59*(4), 369-377. https://link.springer.com/article/10.3103/S0003701X23700020

10. Kumar, N. M., Chopra, S. S., de Oliveira, A. K. V., Ahmed, H., Vaezi, S., Madukanya, U. E., & Castañón, J. M. (2020). Solar PV module technologies. In Photovoltaic Solar Energy Conversion (pp. 51-78). Academic Press. https://www.sciencedirect.com/science/article/pii/B9780128196106000 03X

11. Nema, S., Nema, R. K., & Agnihotri, G. (2010). Matlab/simulink based study of photovoltaic cells/modules/array and their experimental verification. *International Journal of Energy and Environment, 1*(3), 487-500. https://www.academia.edu/download/56701908/IJEE_sn_simulink.pdf

12. Oh, W., Park, J., Jeong, C., Park, J., Yi, J., & Lee, J. (2020). Design of a solar cell electrode for a shingled photovoltaic module application. *Applied Surface Science, 510*, 145420. https://www.sciencedirect.com/science/article/pii/S0169433220301768

13. Oon, L. V., Tan, M. H., Wong, C. W., & Chong, K. K. (2020). Optimization study of solar farm layout for concentrator photovoltaic system on azimuth-elevation sun-tracker. *Solar Energy, 204*, 726-737. https://www.sciencedirect.com/science/article/pii/S0038092X20305181

14. Oufettoul, H., Lamdihine, N., Motahhir, S., Lamrini, N., Abdelmoula, I. A., & Aniba, G. (2023). Comparative performance analysis of PV module positions in a solar PV array under partial shading conditions. *IEEE Access, 11*, 12176-12194. https://ieeexplore.ieee.org/abstract/document/10018222/

15. Pachauri, R. K., Pardhe, M. K., Kazmi, S. A., & Gupta, A. K. (2021). Improved SDK based shade dispersion methodology to achieve higher GMPP of PV systems under shading scenarios. In *2021 IEEE Madras Section Conference (MASCON)* (pp. 1-6). https://ieeexplore.ieee.org/abstract/document/9563589/

16. Shen, L., Li, Z., & Ma, T. (2020). Analysis of the power loss and quantification of the energy distribution in PV module. *Applied Energy, 260*, 114333. https://www.sciencedirect.com/science/article/pii/S0306261919320203

17. Sustainable Energy Development Authority (SEDA). (2022). Photovoltaic Technology. In *Fundamentals of Solar Photovoltaic Technology* (1st ed., p. 104). Malaysia.

18. Tao, M., Fthenakis, V., Ebin, B., Steenari, B. M., Butler, E., Sinha, P., et al. (2020). Major challenges and opportunities in silicon solar module recycling. *Progress in Photovoltaics: Research and Applications, 28*(10), 1077-1088. https://onlinelibrary.wiley.com/doi/abs/10.1002/pip.3316

19. Xu, G., Cai, P., Tu, Y., Kong, H., Ke, Z., Li, Y., ... & Cai, R. (2024). Calibration for Space Solar Cells: Progress, Prospects, and Challenges. *Solar RRL, 8*(6), 2300822. https://onlinelibrary.wiley.com/doi/abs/10.1002/solr.202300822

20. Zhong, T., Zhang, K., Chen, M., Wang, Y., Zhu, R., Zhang, Z., et al. (2021). Assessment of solar photovoltaic potentials on urban noise barriers using street-view imagery. *Renewable Energy, 168*, 181-194. https://www.sciencedirect.com/science/article/pii/S0960148120319704